molecular pharmaceutics

Article

pubs.acs.org/molecularpharmaceutics

Liposome Formation from Bile Salt–Lipid Micelles in the Digestion and Drug Delivery Model FaSSIF$_{mod}$ Estimated by Combined Time-Resolved Neutron and Dynamic Light Scattering

Thomas Nawroth,*[,†] Philipp Buch,[†] Karl Buch,[†] Peter Langguth,[†] and Ralf Schweins[‡]

[†]Institute for Pharmacy and Biochemistry, Biopharmacy and Pharmaceutical Technology, Johannes Gutenberg University, Staudinger Weg 5, D-55128 Mainz, Germany

[‡]Institut Laue-Langevin, DS/LSS, 6 Rue Jules Horowitz, F-38042 Grenoble CEDEX 9, France

ABSTRACT: The flow of bile secretion into the human digestive system was simulated by the dilution of a bile salt–lipid micellar solution. The structural development upon the dilution of the fed state bile model FeSSIF$_{mod6.5}$ to the fasted state bile model FaSSIF$_{mod}$ was investigated by small-angle neutron scattering (SANS) and dynamic light scattering (DLS) in crossed beam experiments to observe small and large structures in a size range of 1 nm to 50 μm in parallel. Because of the physiologically low lipid and surfactant concentrations of 2.625 mM egg-phosphatidylcholine and 10.5 mM taurocholate the sensitivity of the neutron-structural investigations was improved by partial solvent deuteration with 71% D_2O, with control experiments in H_2O. Static experiments of initial and end state systems after 6 days of development revealed the presence of mixed bile salt–lipid micelles of 5.1 nm size in the initial state model FeSSIF$_{mod6.5}$, and large liposomes in FaSSIF$_{mod}$, which represent the late status after dilution of bile secretion in the intestine in the fasted state. The liposomes depicted a size of 34.39 nm with a membrane thickness of 4.75 nm, which indicates medium to large size unilamellar vesicles. Crossed beam experiments with time-resolved neutron and light scattering experiments after fast mixing with a stopped-flow device revealed a stepwise structural dynamics upon dilution by a factor of 3.5. The liposome formation was almost complete five minutes after bile dilution. The liposomes 30 min after dilution resembled the liposomes found after 6 days and depicted a size of 44.56 nm. In the time regime between 3 and 100 s a kinetic intermediate was observed. In a further experiment the liposome formation was abolished when the dilution was conducted with a surfactant solution containing sodium dodecyl sulfate.

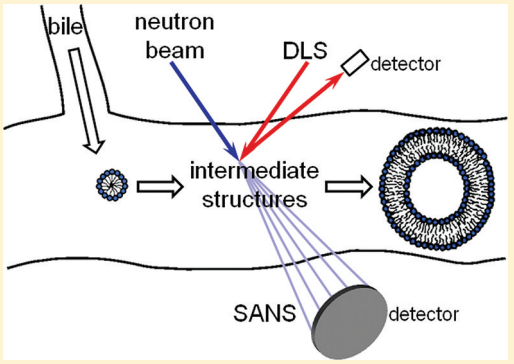

KEYWORDS: *structural dynamics, liposomes, bile micelles, TR-SANS, TR-DLS, stopped-flow*

INTRODUCTION

Pharmacokinetic studies have become time- and cost-intensive. Therefore, one major focus of the pharmaceutical industry is to minimize the number of clinical studies and animal tests. Simulating physiological conditions *in vitro* has gained a critical role in the preformulation step of new drug candidates. As solubility and permeability of a drug are the fundamental determinants of its oral bioavailability, a number of substitute models for both of these parameters have been introduced.

Hydrophobic drugs interact during the delivery and uptake with the bile and lipid systems in the gastrointestinal tract, which have been investigated at high concentrations in structure and dynamics.[1,2] Biorelevant media including FaSSIF and FeSSIF, representing the fasted and the fed state in the upper jejunum, were proposed by Dressman et al.[3] Dissolution studies conducted with these media better predicted the *in vivo* performance of formulations containing poorly soluble drugs compared to the use of compendial media.[4] Through FaSSIF and FeSSIF, dissolution testing has gained a new aspect in the past decade. Besides studying the batch to batch quality of dosage forms, dissolution studies become more and more interesting as a predictive model because relevant physiological parameters are taken into account.

In recent years the compositions of FaSSIF and FeSSIF have been modified to update the simulation in the upper small intestine or to make them usable in permeation studies conducted with cell lines. Kataoka et al.[5] utilized the cell culture medium buffer Hank's balanced salt solution (HBSS) as base for their biorelevant dissolution media, FaSSIF$_{mod}$ and FeSSIF$_{mod6.5}$, and took over the physiological solubilizing substances, sodium taurocholate (NaTC) and egg-phosphatidylcholine (lecithin), in the same concentrations as in FaSSIF and FeSSIF. The dissolution media in their original compositions would destroy the integrity of the cell culture model which Kataoka et al. use in their dissolution/permeation

Received: August 31, 2010
Revised: January 18, 2011
Accepted: October 11, 2011
Published: October 11, 2011

system. With this system two critical parameters of a drug's oral availability, dissolution and permeability, can be determined at the same time.

In a previous study $FaSSIF_{mod}$ was applied as stock solution in solubility and permeation studies.[6] A good *in vitro*−*in vivo* correlation was observed when the *in vitro* solubility and permeability data were combined and compared with the maximum plasma concentrations for five fenofibrate immediate release formulations. The in vitro studies were conducted in $FaSSIF_{mod}$ because this modified biorelevant medium was used in related publications.[7,8]

By investigating the interactions between the surfactant compositions of all formulations and the emulsifying constituents of biorelevant media, it was observed that sodium dodecyl sulfate (SDS) interfered with the vesicle system of $FaSSIF_{mod}$ and therefore its solubilization capacity.[6]

In the present study small-angle neutron scattering (SANS) and dynamic light scattering (DLS) were applied to get a deeper understanding of the colloidal structures in $FaSSIF_{mod}$. It was focused on characterizing the vesicular system in $FaSSIF_{mod}$ which was detected in FaSSIF before[9] and its interaction with a surfactant formulation containing SDS and a surfactant from the class of poloxamers (S2).[6]

The bile salt and phospholipid concentrations in the generally accepted biorelevant media are mean values derived from investigations in human aspirates, which lead to rather static systems compared to the *in vivo* situation. Therefore, the flow of bile secretion into the human digestive system was simulated by the dilution of $FeSSIF_{mod6.5}$ to $FaSSIF_{mod}$. The structural dynamics was studied by a fast mixing dilution technique with a stopped-flow device in combination with synchronous time-resolved neutron and dynamic light scattering (TR-SANS and TR-DLS) in a novel double beam technique. This gives information about the structural conversion between the simulated fed to the fasted state as well as during the transport of bile and food in the upper gastrointestinal system.

EXPERIMENTAL SECTION

Materials. Lecithin (Lipoid EPCS) was purchased from Lipoid GmbH (Ludwigshafen, Germany). NaTC was kindly donated by Prodotti Chimici e Alimentari SpA (Basaluzzo, Italy) via their German agent Alfred E. Tiefenbacher GmbH & Co. KG (Hamburg, Germany). All chemicals were at least of analytical grade and purchased from Sigma-Aldrich (Steinheim, Germany) and Merck-VWR (Darmstadt, Germany). The samples and solutions were sterile filtered after preparation. The physiologic salt buffers HBSS and phosphate-buffered saline (PBS) were purchased as sterile solutions from Invitrogen (Carlsbad, CA).

Preparation of $FaSSIF_{mod}$, $FeSSIF_{mod6.5}$, and Surfactant Solution. As the master solution HBSS including 19.45 mM glucose and 10 mM *N*-(2-hydroxyethyl)piperazine-*N*′-propanesulfonic acid (HEPES) was used (transport medium, TM). $FeSSIF_{mod6.5}$ was based on TM supplemented with NaTC 15 mM and lecithin 3.75 mM. $FaSSIF_{mod}$ was prepared by diluting $FeSSIF_{mod6.5}$ five times with TM.

The surfactant solution for control experiments contained 1 g/L S2 and 0.747 g/L SDS in TM, based on H_2O or 99.75% D_2O. All solutions depicted a pH of 6.5.

Stopped-Flow Mixing. The stopped-flow experiment should simulate the preparation of $FaSSIF_{mod}$ by diluting $FeSSIF_{mod6.5}$ five times with TM. $FeSSIF_{mod6.5}$ had to be prediluted before the time-resolved experiments to c = 10.5 mM NaTC and c = 2.625 mM lecithin, because the syringe volumes of the stopped-flow mixing device allowed only a 3.5 times dilution of $FeSSIF_{mod6.5}$.

The DLS was observed with a ProSpecD 500 projecting DLS optics device from Nanovel (Langenlonsheim, Germany) connected to a single photon detector SIPC-II and a ALV-7001 correlator from ALV (Langen, Germany). The ProSpecD 500 projecting DLS device contained a polarized helium−neon laser of 5 mW power and mode T_{m00} at 638 nm wavelength and revealed a detection volume of 25 × 25 × 400 μm in 70 mm distance from the device front. The data collection and basic evaluation was done with the ALV3 software for Windows-XP. For the time-resolved experiments the data were collected in 30 s frames using the autoscript modus. The samples were investigated in 2 mL autosampler vials from Chromacol Ltd. (Herts, UK), or directly in 10 × 1 mm quartz cuvettes for neutron scattering, purchased from Hellma (Müllheim, Germany).

For the time-resolved experiments the samples were mixed with a modified pressurized air stopped-flow device SFxM20 from HighTech Scientific (Oxford, UK) connected to a SFC220 triple stopped-flow remote controller from Nanovel. A mixing ratio of 1 + 2.5 (prediluted bile salt−lipid solution $FeSSIF_{mod6.5}$: TM or surfactant solution) was selected by the drive-syringes A and B, 1 and 2.5 mL, from Kloehn (Las Vegas, NV). The third channel C of the mixing device (1 mL) was used as visco-elastic brake and drove the stop-syringe D (1 mL) bearing the ready-switch by transfer of a viscous 50% glycerol solution through a thin Teflon tube (0.3 mm) of 20 cm length. The components from syringes A and B, that is, bile salt−lipid micelle solution and buffer, were delivered by Teflon tubings of 0.8 mm inner diameter to an external four-channel Tefzel mixer, which was equipped with a purge valve and a short tubing to the sample cuvette. The sample cuvette was equipped with a bent 0.96 mm steel needle at the side for filling and removal of the used sample after each experiment. For each shot the cuvette was flushed and drained. The filling time was adjusted to 1 s by the visco-elastic brake (syringe C) and the driving air pressure (4 bar). The signal from the stop syringe (sample ready) was amplified and converted to a TTL-pulse with the SFC220 controller and used as trigger signal for starting the data collection of the D11 instrument.

Small-Angle Neutron Scattering. The small-angle neutron scattering (SANS) experiments were done with the improved flux version of the D11 instrument[10] at the high flux reactor of the Institut Laue-Langevin (Grenoble, France). The instrument has now a flux of 9×10^7 N/s·cm^2 at the sample. The scattering profiles were observed at 1.2 and 8 m detector-sample distance and collimation using a position sensitive 128 × 128 pixel ^{3}He-detector. The sample cuvette for the time-resolved experiments and additional cuvettes for static samples and references were located in parallel in the standard sample changer device of the D11 instrument, which can take up to 22 samples.

For the double beam SANS-DLS experiments, the projecting DLS device was mounted on a positioning drive from Isel, Eichenzell, 130° tilted above the sample, which was located together with the mixer, purge valve, and purge syringe and some reference samples in the standard sample changer device of the D11 instrument. The 170° backscattering detection plane of the projecting DLS was located rectangular to the neutron beam-DLS laser plane. The data collection of the

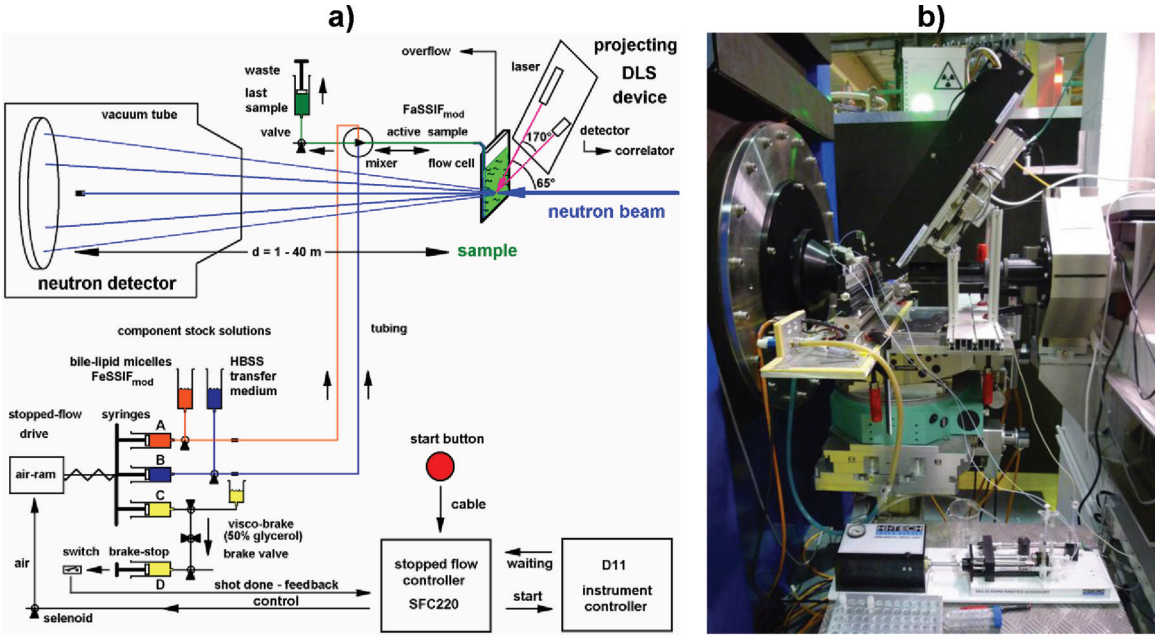

Figure 1. Setup for the structural dynamics investigation of liposome formation by time-resolved neutron and dynamic light scattering: (a) scheme, (b) situation at the instrument ILL-D11.

SANS after the shot ready signal was done with an initial time resolution of 1 s and a logarithmical increase of the frame width by 5.3%/frame.

The experimental setup is shown in Figure 1. A parallel neutron beam of 9% wavelength divergence is delivered to a flat quartz sample cuvette in the D11 instrument. The projecting DLS device containing a helium−neon laser, and the detection unit in backscattering geometry was adjusted to the same sample area from above. The laser focus was adjusted ~300 μm behind the entrance window, which avoids light scattering from windows attached particles.

The neutron data basic evaluation, machine specific corrections, and radial averaging were done with the SANS program package from Ghosh and GRASP from Dewhurst (both online, available at http://www.ill.eu). Further evaluation of SANS and DLS data was done using our programs Kinex-Dacon3 from Nanovel and the datasheet evaluation and plot program SigmaPlot.

Data Evaluation. The scattering profiles were expressed wavelength-independent in terms of the momentum transfer q (scattering vector) which was calculated from the neutron wavelength λ and the half scattering angle θ, according to eq 1. The SANS data were normalized to the neutron flux monitored during the irradiation time. The radius of gyration R_g of the liposomes as well as the bilayer thickness d were obtained by Guinier and Kratky−Porod plots[11−13] of the neutron scattering profiles according to eqs 2 and 3. The radius of gyration R_g is defined as the geometric averaged distance of the scatters from the center of the object. In case of a solid sphere it is by a factor of $(5/3)^{1/2}$ smaller as the outer particle radius r. It is obtained from the leftmost part of the scattering profile, in the Q range where $QR_g < 1$, according to eq 2.

$$q = \frac{4\pi}{\lambda}\sin\theta \tag{1}$$

(scattering vector, momentum transfer)

$$\ln(I(q)) = \ln(I_0) - \frac{R_g^2}{3}q^2 \tag{2}$$

(logarithmic Guinier equation)

$$\ln(I_d(q)) = \ln(I_{do}) - R_d q^2 \tag{3}$$

(logarithmic Kratky−Porod equation)

$$I_d(q) = I(q)\cdot q^2 \tag{4}$$

(thickness scattering profile $I_d(q)$)

$$d = R_d\sqrt{12} \tag{5}$$

(membrane thickness d)

$$s = 2r_m + d \cong 2R_g + d \tag{6}$$

(liposome size s from SANS).

The thickness radius R_d is obtained from the logarithimic evaluation of the thickness profile $I_d(q)$, which is calculated from the middle part of the scattering profile $I(q)$ by multiplication by the thickness factor q^2 according to eq 4. It is linear, if one dimension of the particle is much smaller than the others, for example, in case of a plate or a thin-walled hollow sphere. With eq 5 the thickness of the membrane d is obtained by multiplication of R_d by root of 12.

In case of spherical unilamellar liposomes the radius of gyration R_g is equivalent to the membrane radius r_m.[14] The size s of the liposomes can be estimated by small-angle scattering by eq 6.

The DLS back scattering setup avoids artifacts from multiple scattering.[15] The scattering signal was detected from the scattering object only, that is, without a reference beam in the autobeating mode. The autocorrelation function according to eq 7 reveals the intensity fluctuations in time by varying interparticular interference upon particle motion. In case of moderate particle numbers in the detection volume, ~10^4, ...,

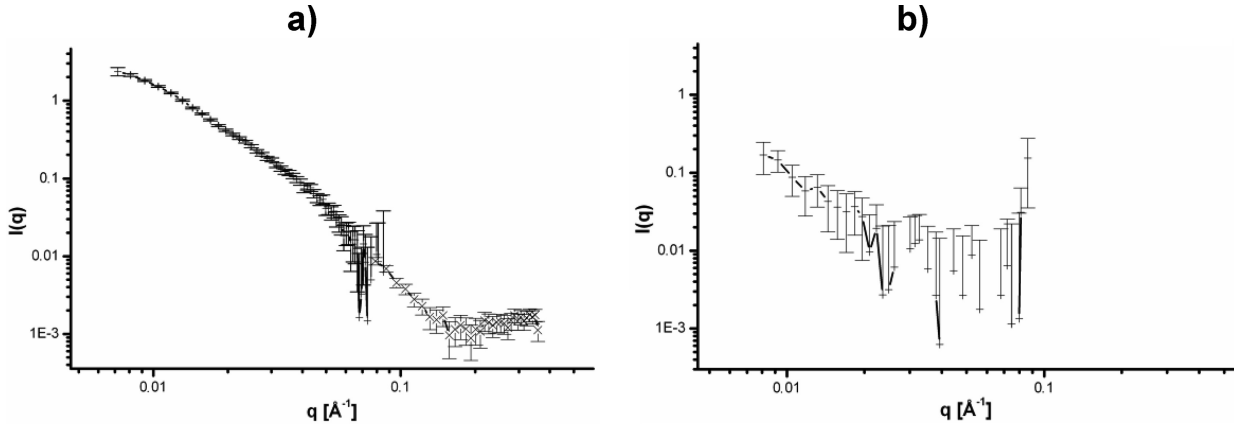

Figure 2. SANS profiles of the bile salt–lipid mixture FaSSIF$_{mod}$ in (a) 71% D_2O and (b) H_2O 6 d after the dilution of FeSSIF$_{mod6.5}$ (end point). The profile was estimated at sample–detector distances of 1.2 m (a) and 8 m (a and b).

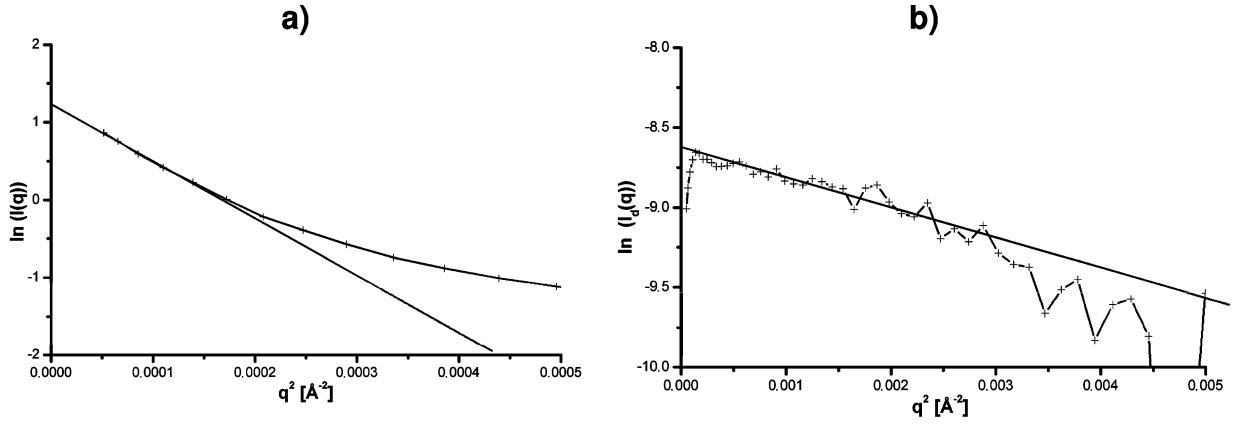

Figure 3. SANS evaluation of liposomes in the bile salt–lipid mixture FaSSIF$_{mod}$ in 71% D_2O 6 d after the dilution of FeSSIF$_{mod6.5}$ (end point): (a) the Guinier plot yields a radius of gyration of R_g = 14.82 ± 0.21 nm; (b) the Kratky–Porod representation indicates a lipid layer thickness of d = 4.75 ± 0.21 nm. The combination yields a liposome size s = 34.39 ± 0.63 nm.

10^6, the correlation time corresponds to the particle diffusion coefficient D. For solutions of moderate concentration, where the particles do not form a crowded network or gel, the average particle radius r is obtained with the Stokes–Einstein relation (eq 8) from the diffusion coefficient D, the solvent viscosity η, and the temperature T. With the ALV software the evaluation was done by automatic iteration using the "regularized fit" function up to the nonweighted distance distributions $S(r)$ (CONTIN method acording to Provencher and Štêpánek[16]), which represent the composition of the scattered light from contributions of particles of different size (populations). In these raw data the large particles are strongly overweighted as compared to mass-weighted particle size distributions.

$$G2(\tau) = C(\tau) = \lim_{M\to\infty} \frac{1}{2M} \int_{t=-M}^{M} I(t) \times I(t+\tau)\mathrm{d}t \quad (7)$$

(autocorrelation function in the measure time M)

$$D = \frac{k_b T}{6\pi\eta r} \quad (8)$$

(Stokes–Einstein diffusion law)

$$C_{m3} = \frac{S(r)}{r^3} \quad (9)$$

(particle mass distribution $C_{m3}(r)$ for solid particles, micelles)

$$C_{m2} = \frac{S(r)}{r^2} \quad (10)$$

(particle mass distribution $C_{m2}(r)$ for liposomes)

$$I_{int} = I_1 \exp[-kt] + I_2(1 - \exp[-kt]) \quad (11)$$

(exponential development of SANS of final product (I_2) from a precursor (I_1) without an intermediate).

The further evaluation to mass-weighted particle size distributions $C_m(r)$ was done due to common scattering laws depicted in eqs 9 and 10: The particle mass as well as the scattering wave amplitude of a single particle is proportional to the number of atoms within. This is for a solid particle proportional to the third power of the radius, but for a hollow sphere as a liposome to the product of second power of the radius and the membrane span, which is constant. The observed intensity is the square of the scattering amplitude value. Thus the mass-weighted solid particle size distribution $C_{m3}(r)$ was estimated by the division of the nonweighted size distributions $S(r)$ by r^3 according to eq 9 in the case of solid particles, for example, micelles. But the mass-weighted size distributions $C_{m2}(r)$ for hollow particle were calculated by the division of $S(r)$ by r^2 according to eq 10 in the case of liposomes, where the membrane span d does not increase with the particle size.

dx.doi.org/10.1021/mp100296w | Mol. Pharmaceutics 2011, 8, 2162–2172

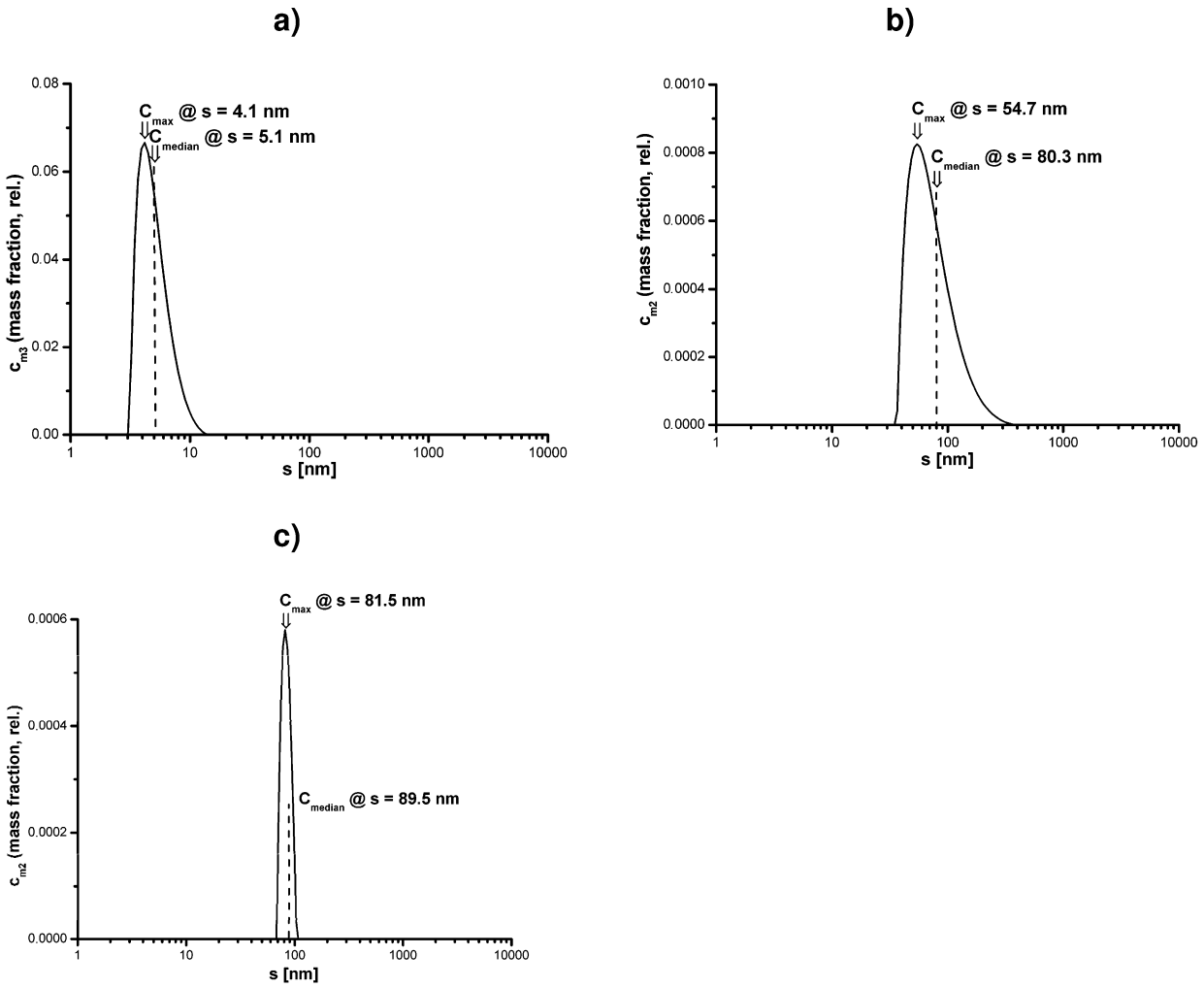

Figure 4. Average size estimations by DLS of: (a) bile salt−lipid micelles in the initial solution $FeSSIF_{mod6.5}$, and liposomes in the bile salt−lipid mixture $FaSSIF_{mod}$ in (b) H_2O and (c) D_2O 6 d after the dilution of $FeSSIF_{mod6.5}$ (end point).

The radius obtained by DLS experiments r_{dls} is the geometric average of the particle main axes including the hydration shell. Thus it is often larger than the radius obtained by other methods, for example, in the case of bulky headgroups in stealth liposomes.[17] Due to the observation of the fluctuations only, backscattering DLS without angle variation has a typical size error of 10−20%.

For the observation of the structural development in the bile salt−lipid system in the small intestine we have adapted the $FeSSIF_{mod6.5}$ model, which is suitable to the physical conditions of a fast mixing system with a stopped-flow device and SANS in double beam experiments as shown in Figure 1. The active sample $FaSSIF_{mod}$ was produced in an external mixer by fast mixing of prediluted bile salt−lipid solution and TM during 1 s and observed during up to 1 h. Static samples were investigated as above, but without mixing in a further cuvette located in the sample changer device (left middle in Figure 1b).

For long structural development time static samples were prepared 6 days before the structural investigation. A homologous sample pair was prepared in H_2O and 71% D_2O systems to improve the particle contrast.[18] A D_2O concentration of only 71% was used to avoid aggregation risk known for some membrane proteins at high glutathione levels and D_2O.

RESULTS

The SANS profiles of the end product $FaSSIF_{mod}$ in 71% D_2O and H_2O are shown in Figure 2 a and b. With the resolution of the experiment, the scattering profiles are equivalent, while the profile of the sample in H_2O is rather noisy.

The evaluation of the neutron scattering of the static $FaSSIF_{mod}$ sample in 71% D_2O by the Guinier representation is shown in Figure 3a. From the plot a radius of gyration of R_g = 14.82 ± 0.21 nm was calculated. Figure 3b depicts the evaluation of the same scattering profile by a Kratky−Porod plot, which yields the thickness of the particle in case of flat particles. The plot indicates a lipid layer thickness of d = 4.75 ± 0.21 nm. The combination of both results according to eq 6 yields a liposome size s = 34.39 ± 0.63 nm.

The 6 day old end product $FaSSIF_{mod}$ sample (diluted) and the initial bile salt−lipid solution $FeSSIF_{mod6.5}$ (concentrated) were investigated by DLS. Figure 4 shows the obtained size distributions in a representation depicting the mass fraction of (a) micelles and (b) liposomes in H_2O and (c) liposomes in D_2O according to eqs 9 and 10, respectively.

With the initial solution $FeSSIF_{mod6.5}$ the particle size distribution in Figure 4a was obtained. The calculated average size of s_{av} = 5.1 nm and most frequent size of s_{max} = 4.1 nm indicates micelles.

The FaSSIF$_{mod}$ end product in H_2O (Figure 4b) and D_2O (Figure 4c) revealed an average particle size of s_{av} = 80.3 and 89.5 nm and a most frequent size of s_{max} = 54.7 and 81.5 nm. This indicates the formation of liposomes in FaSSIF$_{mod}$ from micelles by dilution of the initial solution FeSSIF$_{mod6.5}$.

In a special experiment the liposome formation was prevented by changing the dilution solution for the preparation of FaSSIF$_{mod}$. TM was substituted by a surfactant solution containing a SDS-S2 mixture to further characterize the interactions between emulsifying constituents of biorelevant media and surfactants which had been observed before.[6] Upon dilution the resulting end product (FaSSIF-SDS-S2, FaSSIF$_{SDSS2}$) comprised the same bile salt–lipid concentration compared to FaSSIF$_{mod}$. The static neutron scattering of the samples in 71% D_2O after 6 d development is shown in Figure

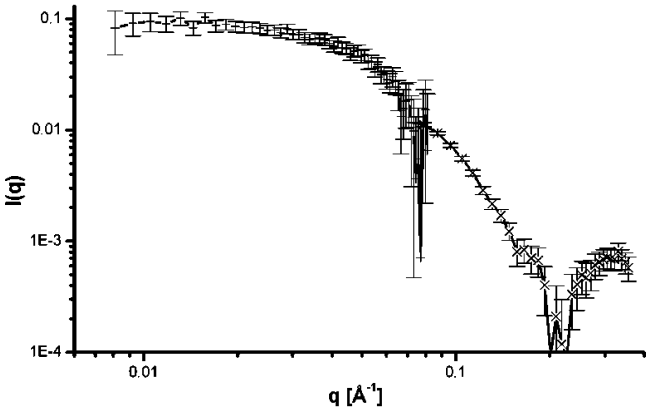

Figure 5. SANS profiles of the surfactant-resolved bile salt–lipid mixture FaSSIF$_{SDSS2}$ in 71% D_2O 6 d after the dilution of FeSSIF$_{mod6.5}$ (end point). The profile was estimated at sample–detector distances of 1.2 and 8 m.

5. The noisy profile of the corresponding H_2O sample (not shown) depicted no additional signal at low q as compared to the contrast enforced D_2O specimen. Thus the profile of the sample in 71% D_2O was evaluated.

The particle size estimation of the surfactant-resolved FaSSIF$_{SDSS2}$ particles in 71% D_2O after 6 days of development by a Guinier representation of SANS is shown in Figure 6. The plot yields a radius of gyration of R_g = 2.96 ± 0.05 nm. The trial

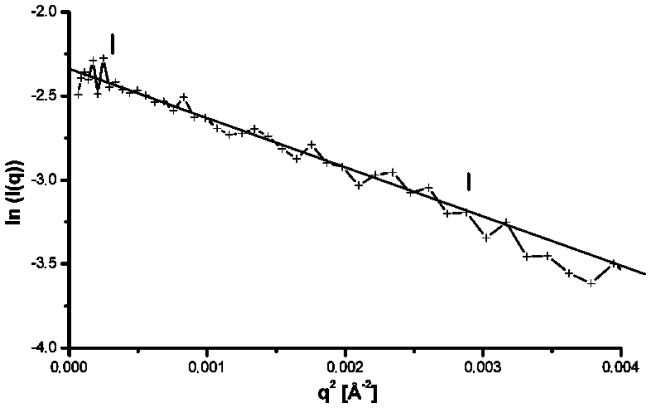

Figure 6. SANS evaluation of micelles in the surfactant-resolved bile salt–lipid mixture FaSSIF$_{SDSS2}$ in 71% D_2O 6 days after the dilution of FeSSIF$_{mod6.5}$ (end point): the Guinier plot yields a radius of gyration of R_g = 2.96 ± 0.05 nm.

of a Kratky–Porod plot yielded no straight line. This indicates the structure of the surfactant-resolved FaSSIF$_{SDSS2}$ particles as micelles.

Figure 7 depicts the investigation of surfactant-resolved FaSSIF$_{SDSS2}$ by DLS. The size distribution was treated as for massive particles according to eq 9. The obtained average

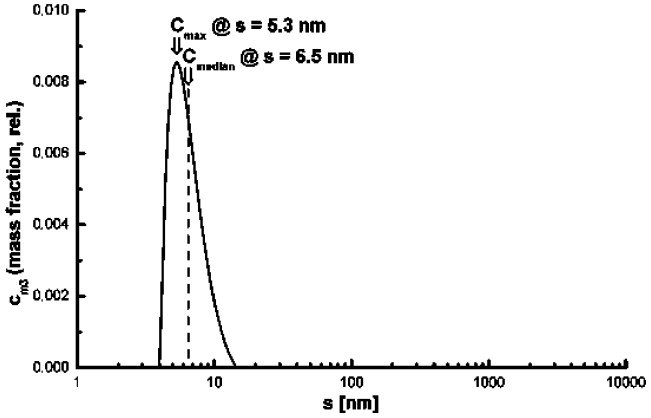

Figure 7. Average size estimation of micelles in the surfactant-resolved bile salt–lipid mixture FaSSIF$_{SDSS2}$ in 71% D_2O 6 d after the dilution of FeSSIF$_{mod6.5}$ by DLS (300 s).

particle size was s_{av} = 6.5 nm, while the most frequent particle size was s_{max} = 5.3 nm.

The structural development of FeSSIF$_{mod6.5}$ to FaSSIF$_{mod}$ in 71% D_2O after dilution by fast mixing was investigated by double beam-time-resolved SANS and DLS. The time-resolved neutron scattering profile is shown in Figure 8 as a 3D plot with logarithmic time resolution. The data of the early time frames

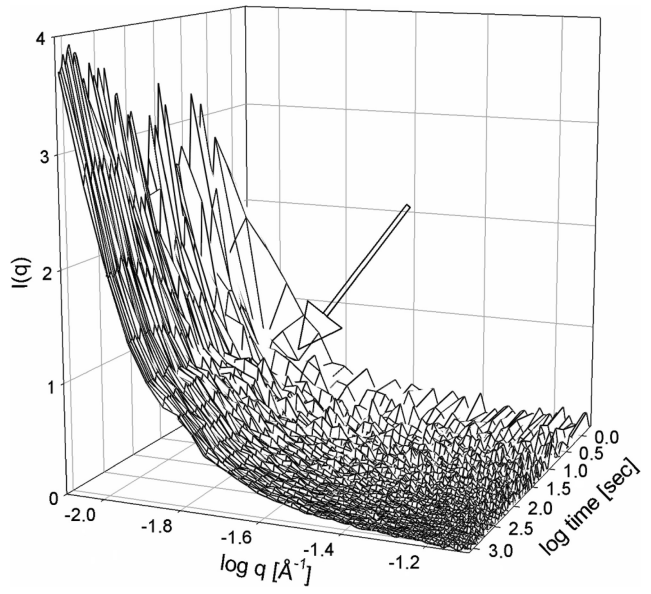

Figure 8. Time-resolved neutron scattering profiles of the bile salt–lipid mixture FaSSIF$_{mod}$ in 71% D_2O upon fast dilution of FeSSIF$_{mod6.5}$ with TM with a stopped-flow device: 3D representation (ln–log) of the development in time after dilution.

are noisy due to the short span (1 s), while the signal at the shot end (front) is improved by the longer frame width (72.7 s). The duration of the experiment was 1389 s. Figure 9 depicts the neutron scattering profile of the last frame, which resulted

dx.doi.org/10.1021/mp100296w | Mol. Pharmaceutics 2011, 8, 2162–2172

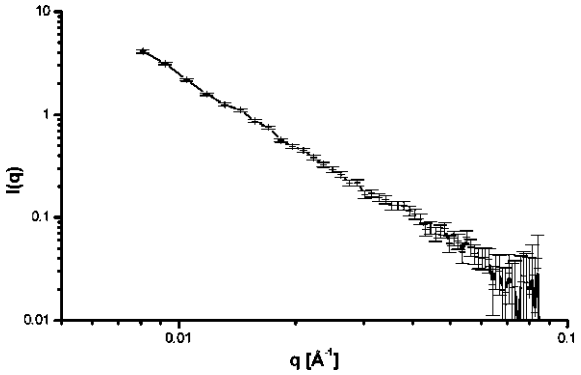

Figure 9. SANS of the bile salt−lipid mixture FaSSIF$_{mod}$ in the last time frame of time-resolved neutron scattering at 1389 s.

from the longest exposure of the shot. The good signal-to-noise ratio of 500 enabled further evaluation.

The evaluation of the neutron scattering profile from the last frame in the time-resolved investigation is shown in Figure 10. The Guinier plot (a) yielded a radius of gyration of R_g = 19.91 ± 0.46 nm. The Kratky−Porod plot (b) contained a noisy linear range, which indicates a lipid layer thickness of about d = 4.74 ± 0.63 nm. This indicates liposomes of a size of s = 44.56 ± 1.55 nm.

For the kinetic evaluation of the time-normalized neutron scattering the integral particle scattering after buffer subtraction $I_{int}(t)$ was estimated according to eq 11. Figure 11a depicts the development of the integral particle scattering of the system in 71% D_2O, after subtraction of the contribution of the buffer, upon time after the concentration jump with logarithmic time scale. The profile consists of three phases: (A) early (t < 3 s), (B) intermediate (3−100 s), and (C) late (>100 s). The late phase revealed a delayed linear behavior in the semilogarithmic plot, shown in Figure 11b. The formation of the late product is described by the constant k_3 = 0.00961 ± 0.00125 s^{-1} ($t_{1/2}$ = 72.1 ± 10.8 s). The initial material depicted a relative scattering intensity of I_1= 557 ± 78, the end product a value of I_2 = 917 ± 10. The calculated exponential function (A−C conversion) is drawn in Figure 11a in green color, in comparison to a simple linear extrapolation of the late phase (black line). The difference between the experimental data and the late exponential behavior was evaluated further as evidence of an intermediate.

The difference signal, experiment signal minus late exponential function, is shown in Figure 12a with logarithmic time scale. The profile depicts the peaklike contribution of an intermediate between 3 and 100 s after the concentration jump, that is, the formation and decay of a transient particle concentration. The kinetic evaluation by a semilogarithmic plot in Figure 12b yielded time constants of k_1 = 0.114 ± 0.025 s^{-1} ($t_{1/2}$ = 6.1 ± 1.7 s) for the formation and k_2 = 0.0178 ± 0.0058 s^{-1} ($t_{1/2}$ = 39.0 ± 18.7 s) for the decay.

The structural development after the concentration jump in the same experiment but analyzed by time-resolved DLS is shown in Figure 13a as a 3D representation. The plot depicts the nonweighted distance distributions $S(r)$ after normalization of the maximum peak height to unity, which is suitable for a comparison of signals from different samples. The development after mixing (back) to equilibrium (front) indicates the transient occurrence of at least three particle populations. The peak shift in the nonweighted time-resolved DLS signal indicates the transformation of particles of 15 nm size to those of 100 nm diameter.

The size distribution at the end of the shot in Figure 13b was weighted to the mass contribution of liposomes according to eq 10. The average size was s_{av} = 99.4 nm, and the most frequent particles had a diameter of s_{max} = 70.7 nm.

DISCUSSION

Considering the various routes of administration for new drug entities, the oral route remains the most common. Besides the permeability, the solubility behavior of a drug is a crucial factor of its oral bioavailability. With the increasing number of poorly soluble active substances in the pharmaceutical industry, the issue of low bioavailability due to solubility-limited absorption is one of the greatest challenges to formulation scientists. Hydrophobic drugs form intermediate complexes with bile and lipids and their nanostructured assemblies in the gastrointestinal system.[19] This interaction is the key for the development of formulations providing sufficient bioavailability of lipophilic drugs.

Although FaSSIF and FeSSIF are simplified models of the gastrointestinal composition, they have been shown to forecast

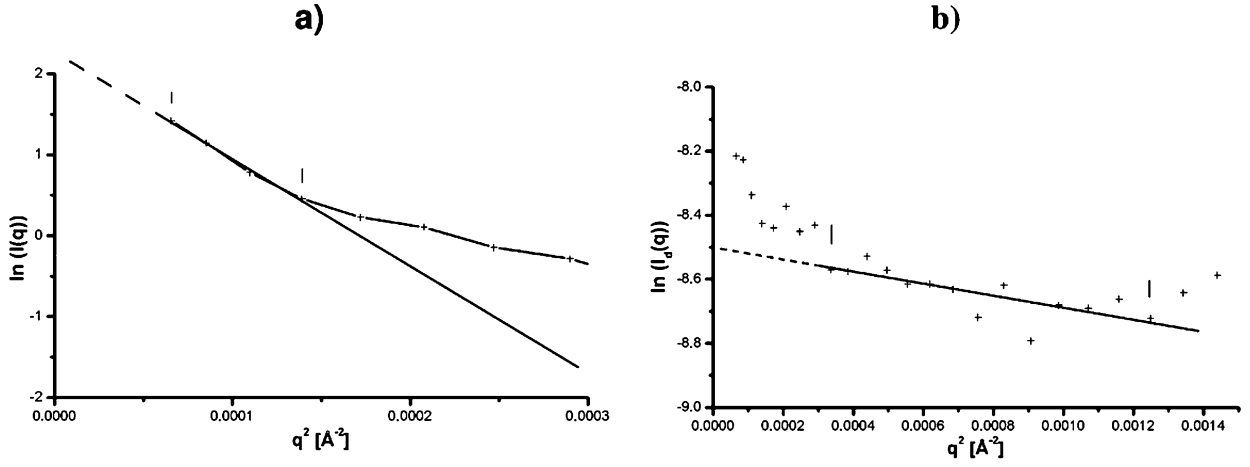

Figure 10. SANS evaluation of liposomes in FaSSIF$_{mod}$ (71% D_2O) at 1389 s (last time frame, 72.7 s duration) upon dilution of the bile salt−lipid mixture FeSSIF$_{mod6.5}$: (a) the Guinier plot yields a radius of gyration of R_g = 19.91 ± 0.46 nm; (b) the Kratky−Porod representation indicates a lipid layer thickness of about d = 4.74 ± 0.63 nm. The combination yields a liposome size s = 44.56 ± 1.55 nm.

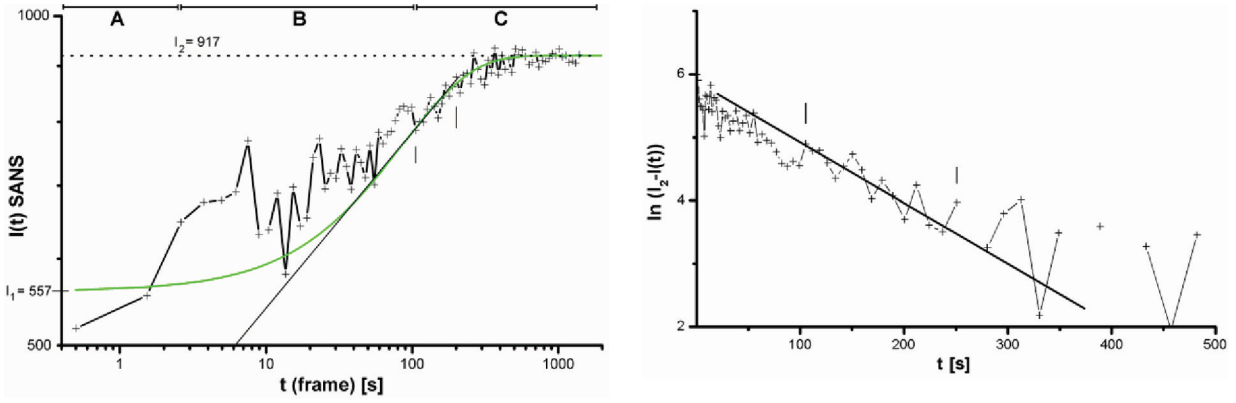

Figure 11. (a) Biphasic development of integral SANS (buffer subtracted) upon time in $FaSSIF_{mod}$ (71% D_2O) after dilution of the bile salt−lipid mixture $FeSSIF_{mod6.5}$. The late development at long time (range C, without intermediate contribution) is extrapolated by a straight line and exponential function (green). (b) Kinetics of liposome formation upon time after dilution of the bile salt−lipid mixture $FeSSIF_{mod6.5}$ to $FaSSIF_{mod}$ (71% D_2O) estimated by semilogarithmic plot of SANS data range C.

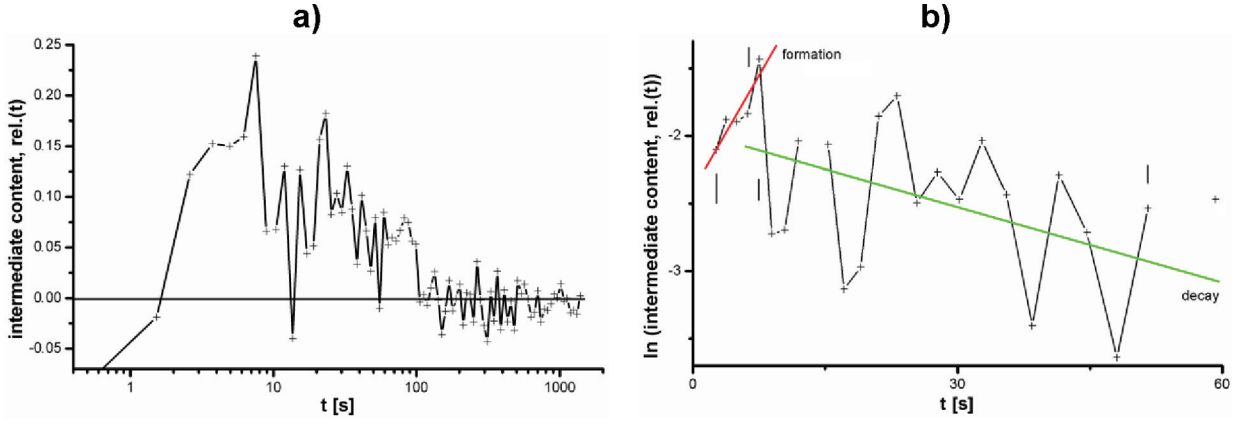

Figure 12. (a) Development of the intermediate signal in integral SANS (buffer subtracted) in $FaSSIF_{mod}$ (71% D_2O) upon time after the dilution of the bile salt−lipid mixture $FeSSIF_{mod6.5}$. (b) Formation and decay kinetics of the bile salt−lipid intermediate upon time after the dilution of the bile salt−lipid mixture $FeSSIF_{mod6.5}$ to $FaSSIF_{mod}$ (71% D_2O) estimated by semilogarithmic plot of SANS data range B (Figure 11a).

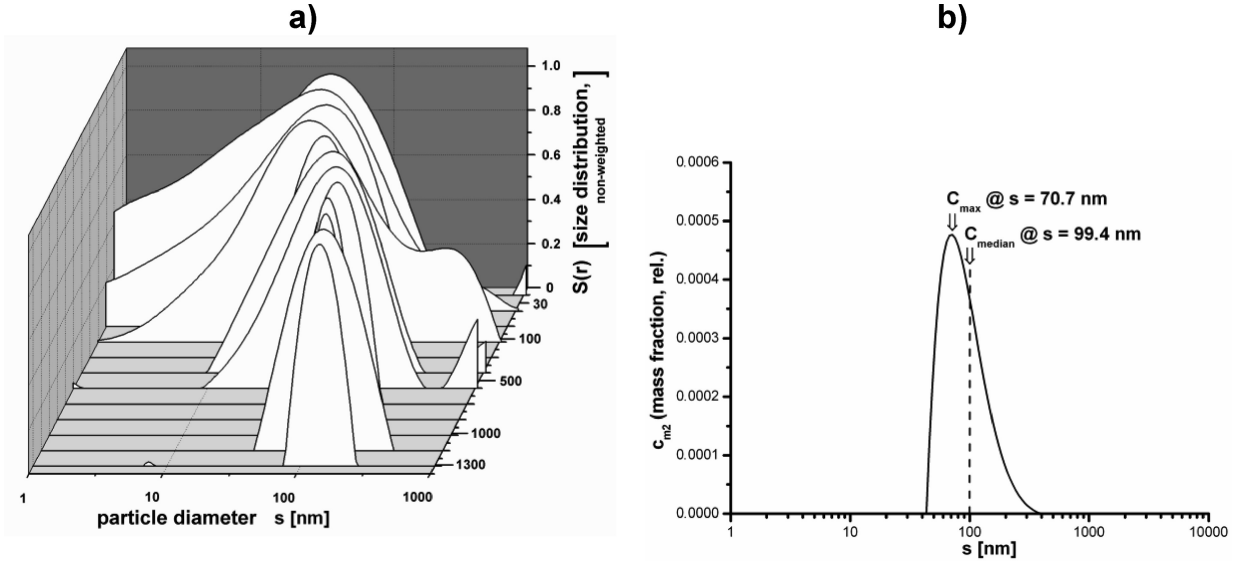

Figure 13. (a) Particle size distribution (nonweighted, normalized to 1) in TR-DLS upon time after dilution of the bile salt−lipid mixture $FeSSIF_{mod6.5}$ to $FaSSIF_{mod}$ (71% D_2O) shows a peak shift from a broad double peak of small particles to unique large particles. Between 30 and 120 s after the concentration jump an intermediate of 15−110 nm size occurs. (b) Mass-weighted average size distribution $C_{m2}(s)$ of liposomes in the bile salt−lipid mixture $FaSSIF_{mod}$ in 71% D_2O at the end of time development after dilution (front in A), obtained with a TR-DLS frame duration of 300 s.

dx.doi.org/10.1021/mp100296w | *Mol. Pharmaceutics* 2011, 8, 2162−2172

the effect of food on absorption of poorly soluble drugs and have found application in the pharmaceutical industry to evaluate new drugs and dosage forms. Over the years the biorelevant media have been slightly adjusted to improve the predictions of *in vivo* performance or to render them suitable in permeation studies conducted with cell lines.[5] In a previous study it has been shown that a continuous dissolution/permeation system combined with the modified biorelevant dissolution media, $FaSSIF_{mod}$ and $FeSSIF_{mod6.5}$, was able to predict the *in vivo* performance in rats of solid oral dosage forms containing the poorly soluble and highly permeable drug fenofibrate.[7]

In a further study it was observed that SDS interfered with the vesicular drug solubilizing system of $FaSSIF_{mod}$ and antagonized its solubilization capacity with regards to fenofibrate.[6] This study provides a deeper characterization of the colloidal structures in the bile salt−lipid mixture developed by this interference with SDS via SANS. Furthermore not only the colloidal structures of $FeSSIF_{mod6.5}$ and $FaSSIF_{mod}$ through static measurements but also the structural development after dilution of $FeSSIF_{mod6.5}$ to $FaSSIF_{mod}$ were investigated. The dilution of $FeSSIF_{mod6.5}$ to $FaSSIF_{mod}$ is both the common preparation method of $FaSSIF_{mod}$ and a simulation of the concentrated bile's fate upon secretion into the small intestine and subsequent transport (Figure 14). The simulation of the fasted state by $FaSSIF_{mod}$ is relevant for the uptake of drugs, which are administered on an empty stomach.

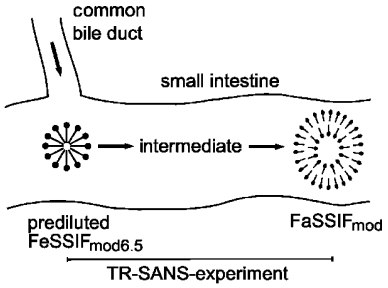

Figure 14. Structural dynamics scheme of liposome formation upon dilution of the bile salt−lipid mixture $FeSSIF_{mod6.5}$ with subsequent gastrointestinal transport simulating the fasted state.

The structures of micelles, mixed micelles, and membrane structures of surfactant−lipid−drug systems may vary between the lower nanometer and the micrometer scale. Leng et al.[2] reported the formation of small and large disk-like mixed lecithin-bile micelles in a sequence after dilution in a more concentrated model system. A combination of neutron and dynamic light scattering is capable of simultaneous detection of those particles and mixtures. This covers a combined size range of 1 nm to 50 μm with high precision of the SANS range up to 100 nm (at 6 Å wavelength and 8 m distance) and moderate error of 10−20% in the DLS range. Simultaneous SANS-DLS experiments in the double-beam technique are mandatory, if the lipid−surfactant system undergoes dynamic transitions, or if the sensitive structures are unstable. With the current work we have established a synchronous time-resolved double beam SANS-DLS technique with sample preparation by fast mixing with a stopped-flow device. The limit in time resolution of 1 s for the SANS investigation and 30 s for the DLS test was given by the technical conditions. Especially the low concentrations of lipid and surfactant were given by the pharmaceutical $FaSSIF_{mod}$/$FeSSIF_{mod6.5}$ system,[5] which is much lower as compared to earlier investigations of the physical-chemical behavior of concentrated bile−lipid systems.[20,21] The biological relevance of the study is limited to the initial phase of bile action, that is, the first 10 min after secretion and dilution, where the detergent−lipid system is not changed significantly by material uptake and lipolytic enzyme activity. At a later stage the formed liposomes will be destroyed by conversion of the lipids to lysolipids and subsequent uptake. A more complete description of the process would require an extended study in a physiologic digestion model.

The SANS signal-to-noise ratio of the dilute $FaSSIF_{mod}$/$FeSSIF_{mod6.5}$ systems was improved by partial solvent deuteration. The D_2O content was limited to 71% to prevent a possible change of sensitive aggregation behavior at a high deuteration level.[22] The comparison of the scattering profile of $FaSSIF_{mod}$ with the equivalent solution in H_2O in Figure 2 revealed no significant difference, despite the better signal quality of the D_2O sample. Thus the time-resolved investigation of the structural dynamics after a concentration jump was done with samples in 71% D_2O buffer.

The end product of the dilution of $FeSSIF_{mod6.5}$ to $FaSSIF_{mod}$ after 6 days of development was investigated by static SANS and DLS. The neutron scattering revealed a scattering profile typical for unilamellar liposomes (Figure 2a). The combined results of Guinier and Kratky−Porod plots yielded a size of 34 nm for these large unilamellar liposomes (LUV), similar to those detected in more concentrated systems in the literature.[23] The size distribution of the same system estimated by DLS revealed a larger average particle diameter of 80 nm in H_2O (Figure 4b) and 90 nm in D_2O (Figure 4c). This includes the hydration shell, but possibly a part of the broad size distribution was not seen by the SANS experiment due to the limitation in the q-range. The improvement of the lowest q-limit at a sample distance of more than 36 m, possible at the new D11 instrument, was not used as it would have abolished the possibility for time-resolved experiments by intensity reasons.

The investigation of the more concentrated initial solution $FeSSIF_{mod6.5}$ by DLS in Figure 4a indicated small particles of a diameter of 5.1 nm only. As this is too small for the formation of an aqueous lumen, these are micelles, as described for similar and more concentrated systems in the literature.[9]

As a test for the surfactant dependence of the $FeSSIF_{mod6.5}$/$FaSSIF_{mod}$ system the dilution of $FeSSIF_{mod6.5}$ was done with a surfactant mixture of S2 and SDS. The neutron scattering and DLS of this surfactant system is shown in Figures 5−7. Both methods indicate small particles instead of liposomes, which are formed in the absence of those surfactants.[6] A Kratky−Porod representation of the SANS data (not shown) contained no linear range. Thus no aqueous lumen was detected. The assumption of spherical particles yields a particle size of $s = R_g \times (5/3)^{1/2} = 3.8$ nm. The value is consistent with the particle size distribution from 3 to 14 nm estimated by DLS (Figure 7) with an average size of $s_{av} = 6.5$ nm. Thus the surfactant-resolved bile salt−lipid particles are micelles.

The time-resolved neutron scattering profiles in Figure 8 show the structural development of the freshly prepared $FaSSIF_{mod}$ in the first 23 min after dilution from $FeSSIF_{mod6.5}$ by a factor of 3.5. The time resolution (frame width) increased logarithmically by a factor of 1.053 per frame from 1 to 72.7 s at the end of the shot. Thus the early scattering curves are rather noisy and resemble that of taurocholate micelles from literature.[23] In the subsequent time range of 3 to 100 s (log ~1.5) a temporal peak appeared, which is identified as dynamic

intermediate below. At long time (front) the profile developed to a stable signal of large particles.

For a clearer view the last frame of the film is depicted in Figure 9. It resembles that of the 6 days old $FaSSIF_{mod}$ shown in Figure 2a. Also the size estimation of the material in the last film frame in Figure 10a yielded a radius of gyration of R_g = 20 nm, which is a similar value of the 6 days old preparation (15 nm). The estimation of the membrane span by a tentative Kratky–Porod plot in Figure 10b was rather noisy, due to the short exposition time. Nevertheless the obtained coarse value of $d = 4.74 \pm 0.63$ nm is comparable to that of the static sample of d = 4.75. The results indicate that the $FaSSIF_{mod}$ solution contains already 23 min after preparation equivalent particles as after 6 days development, that is, large unilamellar liposomes, LUV.

For the kinetic analysis of the time-resolved neutron scattering, the total particle scattering signal after buffer subtraction was integrated. The component analysis was done by conventional subtraction of the kinetic contributions. This simple but descriptive evaluation was possible because the time constants of the three subprocesses differed significantly, by factors of 1.85 (k_2/k_3) and 6.4 (k_1/k_2), while in more complicated cases a single value decomposition may be applied. The time-dependent profile of the integral scattering consists of three phases, which are depicted as A, B, and C in Figure 11a. In the last period C the final product LUV is formed in an exponential process. The formation kinetics of this is analyzed in Figure 11b by a semilogarithmic plot. As a result a half formation time of 72 s and the initial scattering rate were estimated. The extrapolated exponential formation curve for short time is shown in Figure 11a additionally. In the initial phases A and B up to 100 s after mixing the integral scattering signal showed a significant deviation from the late product contribution. The initial scattering signal up to 2 s corresponds to the scattering of the freshly diluted solution of micelles. In the time regime between 3 and 100 s (phase B) an extra signal occurred. This is seen well in the difference signal between experimental curve and the extrapolated late product contribution depicted in Figure 12a. Obviously a metastable intermediate is formed during the first 10 s after mixing. It vanishes during the first 2 min of the shot. The kinetic analysis of intermediate formation and decay by a semilogarithmic plot of the difference signal is depicted in Figure 12b. With the limited resolution of the experiment the formation of the intermediate occurs with a half formation time of 6 s. The half-life time for the decay was 39 s.

The formation of the late product LUV is clearly detected by the DLS method through the peak shift of the unweighted size distribution in Figure 13a in the time regime >100 s. The investigation of the final product during 300 s shown in Figure 13b as the mass weighted size distribution yielded an average particle size of 99 nm and a most frequent size of 71 nm. These values are comparable to the estimation by SANS, if one takes into account that the DLS size analysis includes the hydration shell and the limitation of the SANS profile at low scattering vector q, which is equivalent to a large particle cutoff. The occurrence of the intermediate is in the DLS profile visible in the short time range, that is, in the first four frames up to 120 s.

For the identification of the observed nanoparticulate species a comparison with the detailed study of more concentrated lecithin–bile systems in the literature is helpful. Obviously the sequence of the structure conversions in the physiologic $FaSSIF_{mod}/FeSSIF_{mod6.5}$ system resembles a part of the conversion observed by Leng et al.[2] A stacking was not observed. The transient intermediate in this study is obviously equivalent to the large disk micelles found by Leng et al., as indicated by the temporal sequence, that is, the last step preceding the formation of liposomes. For other mixed micelles in the chemical and temporal equilibrium the structures were investigated extensively in the literature.[9,24] The intermediate micelles may play a role for drug uptake by solubilizing hydrophobic drugs, leading to an enforced uptake in a chain of subsequent carrier–drug structures in the digestive system.

AUTHOR INFORMATION

Corresponding Author

*Mailing address: Johannes Gutenberg University, Institute for Pharmacy and Biochemistry, Biopharmacy and Pharmaceutical Technology, Staudinger Weg 5, D-55128 Mainz, Germany. E-mail: nawroth@uni-mainz.de. Phone: +49-6131-3923416. Fax: +49-6131-3925021.

ACKNOWLEDGMENTS

We are thankful for the support from the Bundesministerium für Forschung und Technologie (BMBF, Grant No. 05KS7UMA) and the Institute Laue-Langevin, Grenoble, France.

REFERENCES

(1) Hjelm, R. P. Jr.; Thiyagarajan, P.; Alkan-Onyuksel, H. Organization of phosphatidylcholine and bile salt in rodlike mixed micelles. *J. Phys. Chem.* **1992**, *96* (21), 8653–8661.

(2) Leng, J.; Egelhaaf, S. U.; Cates, M. E. Kinetics of the Micelle-to-Vesicle Transition: Aqueous Lecithin-Bile Salt Mixtures. *Biophys. J.* **2003**, *85* (3), 1624–1646.

(3) Galia, E.; Nicolaides, E.; Horter, D.; Lobenberg, R.; Reppas, C.; Dressman, J. B. Evaluation of various dissolution media for predicting in vivo performance of class I and II drugs. *Pharm. Res.* **1998**, *15* (5), 698–705.

(4) Dressman, J. B.; Reppas, C. In vitro-in vivo correlations for lipophilic, poorly water-soluble drugs. *Eur. J. Pharm. Sci.* **2000**, *11* (2), S73–80.

(5) Kataoka, M.; Masaoka, Y.; Sakuma, S.; Yamashita, S. Effect of food intake on the oral absorption of poorly water-soluble drugs: in vitro assessment of drug dissolution and permeation assay system. *J. Pharm. Sci.* **2006**, *95* (9), 2051–61.

(6) Buch, P.; Holm, P.; Thomassen, J. Q.; Scherer, D.; Branscheid, R.; Kolb, U.; Langguth, P. IVIVC for Fenofibrate Immediate Release Tablets Using Solubility and Permeability as In Vitro Predictors for Pharmacokinetics. *J. Pharm. Sci.* **2010**, *99* (10), 4427–4436.

(7) Buch, P.; Langguth, P.; Kataoka, M.; Yamashita, S. IVIVC in oral absorption for fenofibrate immediate release tablets using a dissolution/permeation system. *J. Pharm. Sci.* **2009**, *98* (6), 2001–9.

(8) Buch, P.; Holm, P.; Thomassen, J. Q.; Scherer, D.; Kataoka, M.; Yamashita, S.; Langguth, P. IVIVR in oral absorption for fenofibrate immediate release tablets using dissolution and dissolution permeation methods. *Pharmazie* **2011**, *66*, 1.

(9) Okazaki, A.; Mano, T.; Sugano, K. Theoretical dissolution model of poly-disperse drug particles in biorelevant media. *J. Pharm. Sci.* **2008**, *97* (5), 1843–1852.

(10) Lindner, P.; Schweins, R. The D11 Small-Angle Scattering Instrument: A New Benchmark for SANS. *Neutron News 21*, (2), 15-18.

(11) Guinier, A. La diffraction des rayons X aux tres petits angles; application a l'etude de phenomenes ultramicroscopiques. *Ann. Phys. (Paris)* **1939**, *12*, 161–237.

(12) Porod, G. Die Abhängigkeit der Röntgen-Kleinwinkelstreuung von Form und Grösse der kolloiden Teilchen in verdünnten Systemen. IV. *Acta Phys. Austriaca* **1948**, *2*, 255–292.

(13) Kratky, O. X-ray small angle scattering with substances of biological interest in diluted solutions. *Prog. Biophys.* **1963**, *13*, 105−173.
(14) Nawroth, T.; Conrad, H.; Dose, K. Neutron small angle scattering of liposomes in the presence of detergents. *Physica B* **1989**, *156*, 477−480.
(15) Peters, R.; Georgalis, Y.; Saenger, W. Accessing lysozyme nucleation with a novel dynamic light scattering detector. *Acta Crystallogr.* **1998**, *54* (5), 873−877.
(16) Provencher, S. W.; Štêpánek, P. Global analysis of dynamic light scattering autocorrelation functions. *Part. Part. Syst. Charact.* **1996**, *13* (5), 291−294.
(17) Hofmann, A. M.; Wurm, F.; Huehn, E.; Nawroth, T.; Langguth, P.; Frey, H. Hyperbranched polyglycerol-based lipids via oxyanionic polymerization: toward multifunctional stealth liposomes. *Biomacromolecules* **2010**, *11* (3), 568−574.
(18) Zackrisson, M.; Stradner, A.; Schurtenberger, P.; Bergenholtz, J. Small-angle neutron scattering on a core-shell colloidal system: a contrast-variation study. *Langmuir* **2005**, *21* (23), 10835−10845.
(19) MacGregor, K. J.; Embleton, J. K.; Lacy, J. E.; Perry, E. A.; Solomon, L. J.; Seager, H.; Pouton, C. W. Influence of lipolysis on drug absorption from the gastro-intestinal tract. *Adv. Drug Delivery Rev.* **1997**, *25*, 33−46.
(20) Mazer, N. A.; Benedek, G. B.; Carey, M. C. Quasielastic light-scattering studies of aqueous biliary lipid systems. Mixed micelle formation in bile salt-lecithin solutions. *Biochemistry* **1980**, *19* (4), 601−615.
(21) Walter, A.; Vinson, P. K.; Kaplun, A.; Talmon, Y. Intermediate structures in the cholate-phosphatidylcholine vesicle-micelle transition. *Biophys. J.* **1991**, *60* (6), 1315−1325.
(22) Lo Nostro, P.; Stubicar, N.; Chen, S. H. Isotopic effect in phase separation of dioctanoylphosphatidylcholine/water micellar solutions. *Langmuir* **1994**, *10* (4), 1040−1043.
(23) Long, M. A.; Kaler, E. W.; Lee, S. P. Structural characterization of the micelle-vesicle transition in lecithin-bile salt solutions. *Biophys. J.* **1994**, *67* (4), 1733−1742.
(24) Small, D. M.; Penkett, S. A.; Chapman, D. Studies on simple and mixed bile salt micelles by nuclear magnetic resonance spectroscopy. *Biochim. Biophys. Acta* **1969**, *176* (1), 178−89.